2006

Comparison of Viscous Damping in Unsaturated Soils, Compression and Shear

Paul Michaels
Boise State University

doi: 10.1061/40802(189)43

Comparison of Viscous Damping in Unsaturated Soils, Compression and Shear

Paul Michaels, PE[1] Member ASCE

[1]Associate Professor, Boise State University, 1910 University Drive, Boise, Idaho 83725 <pm@cgiss.boisestate.edu> 208 426-1929

Abstract

Geophysical down-hole surveys can be used to measure the small strain dynamic properties of soils by the effects these properties have on wave propagation. The relevant effects include amplitude decay (corrected for beam divergence) and velocity dispersion. In this paper, down-hole data collected during the GeoInstitute's Denver 2000 field day are presented and analyzed as a Kelvin-Voigt solid. Findings for these unsaturated soils include viscous damping and stiffness which differ significantly for shear and compressional waves. A strong viscous damping is observed in compression, but weak damping is presented in shear. Lumped parameter constitutive models are discussed which mathematically represent the soil dynamics.

It appears that, in the case of unsaturated soils, the relatively low level of viscous damping in shear may be explained by the low mass of the air in the pores. That is, it is difficult for inertial decoupling to occur between the soil frame and the pore fluid when the pore fluid (air) is of such low density. Thus, a pore fluid in coupled motion with the frame can not produce significant viscous drag. On the other hand, large viscous damping is observed for compressional waves. This larger damping may be due to the larger relative motions between air and frame which can be forced by compression of the frame matrix. These observations may be relevant in areas such as the design of driven piles and the estimation of potential for damages from vibrations due to construction.

Introduction

As one of the participants in the GeoInstitute's Denver 2000 field day, the author collected down-hole data in an unsaturated granular soil. It was a unique opportunity since other participants measured related soil properties by different methods in the same general vicinity. These included ConeTec direct push surveys as well as surface

doi: 10.1061/40802(189)43

wave demonstrations by Olson Engineering. The field site was at the Asphalt Recycling and Stabilization Inc. (ARS) quarry. The author demonstrated a method by which the soil stiffness and damping properties (Kelvin-Voigt constitutive model) could be determined. These soil properties are derived from measurements of seismic wave velocity and amplitude decay as a function of frequency (Michaels, 1998).

The ConeTec demonstration was conducted about 100 meters from the author's down hole survey, and produced soil behavior types (SBT) which indicated a silty sand layer about 4.6 meters thick over a gravely sand which extended to depth of about 9 or 10 meters. Differences in ground elevation were not surveyed, and the distance between the two sites was large enough to prevent more than a qualitative comparison between the two locations.

The Olson Engineering surface wave demonstration was closer, perhaps within 50 meters to the down-hole work. Handouts of Olson's analysis indicated a shear-wave velocity profile that varied between 140 m/s and 230 m/s (0 to 3 meters depth) ending with a constant value of 230 m/s (3 to 6 meters depth). Olson and the author employed different sources. Since our sources were different, the source spectra were also different. Spectral plots handed out by Olson indicated that frequencies used in the SASW inversion extended from about 20 to 280 Hz. The author's down-hole source produced a spectral content from about 10 to 100 Hz, with the most reliable data between 20-80 Hz. The author's hammer delivered blows at 135 degrees from the vertical and is shown in Figure 1.

Figure 1. Hammer source used in down-hole survey

Also shown in the Figure 1 is the stick-up of casing (2.5 inch PVC, schedule 40) and the GeoStuff BHG-2 down-hole 3-component geophone, clamped by a worm driven bowspring. The source is nailed to the soil (0.35 m south of the hole) and the hammer can be pivoted to strike blows from opposing directions. Typically, 3 to 5 blows are stacked from each direction at any depth station and stored as two separate recordings. Subtraction of recordings enhances shear waves, addition of recordings

doi: 10.1061/40802(189)43

enhances compressional waves. Principal component analysis is used to determine the down-hole tool orientation and is described in Michaels (2001). The geophone elements were 14 Hz velocity phones, and a 3 component stationary reference phone was planted 0.6 meters south of the source. The purpose of the reference phone is to provide data to correct for minor variations in the source waveform and triggering. Triggering of the Bison engineering seismograph was by contact closure (between the wired hammer head and the aluminum covered strike plate.

Waveform Data

Figure 2 shows horizontal and vertical component waveform data collected down-hole on the 8th of August, 2000. The horizontal component data were rotated to align with the source polarization (parallel to the 1m source beam) and the vertical component data are taken simply from the single vertical component.

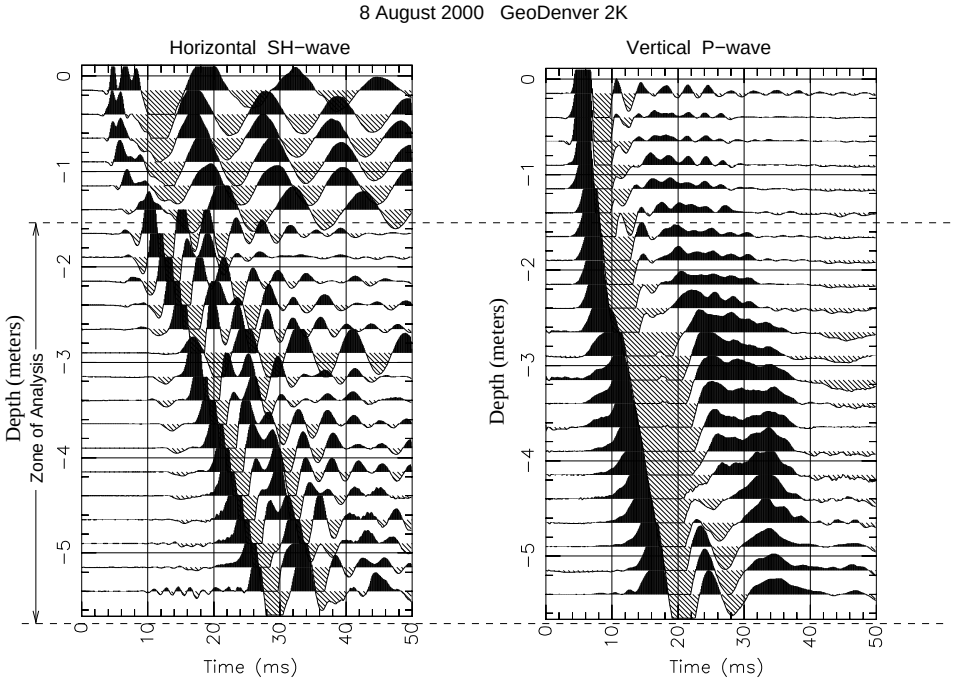

Figure 2. Horizontal and vertical component waveform data.

Data were collected every 0.25 meters, from the bottom of the hole upward. The sample interval was .0001 seconds. Only the first .05 seconds of a 0.5 second recording is shown to display the direct arrival waves with the best clarity. The amplitudes have been rescaled at each depth station by the L2 norm of the signal for that depth. Since true amplitudes decay rapidly with depth and distance propagated, this is the best way to present the waveforms in a single display. The bore hole did not appear to be well coupled to the soil in the first 1.5 meters from the surface. This view was formed by observing poor coherence and a high noise level, especially in

doi: 10.1061/40802(189)43

the horizontal motion (observe the persistent ringing in the horizontal data above 1.5 meters depth). An additional consideration is that surface waves dominate both the horizontal and vertical components at the surface, close to the source. For that reason, only the data from 1.5 to 6.0 meters depth is presented in the analysis which follows. This deeper data presented consistent and coherent wave fields which one would expected for body waves propagating in the soil.

Viscoelastic Analysis

Under the Kelvin-Voigt (KV) constitutive model, both phase velocity and amplitude decay are functions of frequency. The author's analysis method is to jointly invert phase velocity dispersion and inelastic decay observed over a range of frequencies. Velocity dispersion is computed in the time domain. Narrow band (2 Hz) filtered versions of the data are aligned in a depth window using trial velocities. For each alignment velocity, a semblance is computed (objective function to be maximized). A golden section search determines the best velocity for that frequency band. Amplitude decay is observed from the amplitude (after correction for beam divergence) of each filtered version of the data for each depth in the depth window. A least squares linear fit to the logarithmic amplitude decay with depth is performed at each frequency. The slope of that linear solution is the determined decay value for that frequency. A least squares inversion jointly solves for the two coefficients of the 1-D inelastic wave equation (Michaels, 1998). The governing wave equation is

$$\frac{\partial^2 u}{\partial t^2} = C_1 \frac{\partial^2 u}{\partial x^2} + C_2 \frac{\partial^3 u}{\partial t \partial x^2} \quad , \qquad (1)$$

where ***u*** is particle displacement, ***x*** is the direction of wave propagation, and ***t*** is time. The stiffness coefficient is C_1 (m^2/s^2) and the damping coefficient is C_2 (m^2/s). The method is robust when done over a large enough depth window. Effects associated with scattering, mixed or multiple wave fields within the aperture, and near-field waves tend to average out over intervals greater than a few meters. The reader is cautioned not to interpret individual measurements of velocity or decay at any one frequency, as this may be misleading. Rather, the reader should focus on the joint inversion results (C_1 and C_2) which are determined statistically by the data's presentation of Kelvin-Voigt specific behavior.

Figure 3 plots the measured velocity dispersion and amplitude decay for both the P-wave and SH-wave data collected on 8 August, 2000. The depth range analyzed extended from 1.5 to 6 meters depth. Error bars are for 95% confidence limits. The results for the vertical component signals, labeled P-wave, are shown in Figure 3 (a) and (b). The results for the horizontal component signals, labeled SH-wave are shown in c) and d) of the same figure. The reader is urged to observe the solid curves which are computed from the solutions for C_1 and C_2. Note that, for example, the solid velocity curve for P-waves is always faster than the solid curve for S-waves.

doi: 10.1061/40802(189)43

We note that the velocity variation with frequency is significantly greater in the case for the P-wave data. Consistent with that observation, the variation of amplitude decay with frequency is also very much larger in the case for P-waves than for SH-waves. Further, the response is nearly elastic for SH-waves, the propagating wavelet largely retains its shape as the wave propagates. For P-waves, the propagating wavelet stretches its shape with distance propagated, consistent with KV damping. In other words, the damping of P-waves is greater than for SH-waves.

The least squares solution for the wave equation coefficients, C_1 and C_2 are given for the two cases (compression and shear) in Table 1. Note that the damping, C_2, for compression is about 40 times greater than for shear. Confidence limits are for 95%.

The shear-wave velocity solution shown in Figure 3(c) varies from a low of about 245.45 m/s to a high of 245.48 m/s. This extremely low level of dispersion is due to the minimal damping in shear. The average shear velocity magnitude is in general agreement with the analysis from the Olson Engineering SASW survey conducted about 50 meters distant from the borehole. The GeoDenver attenuation is

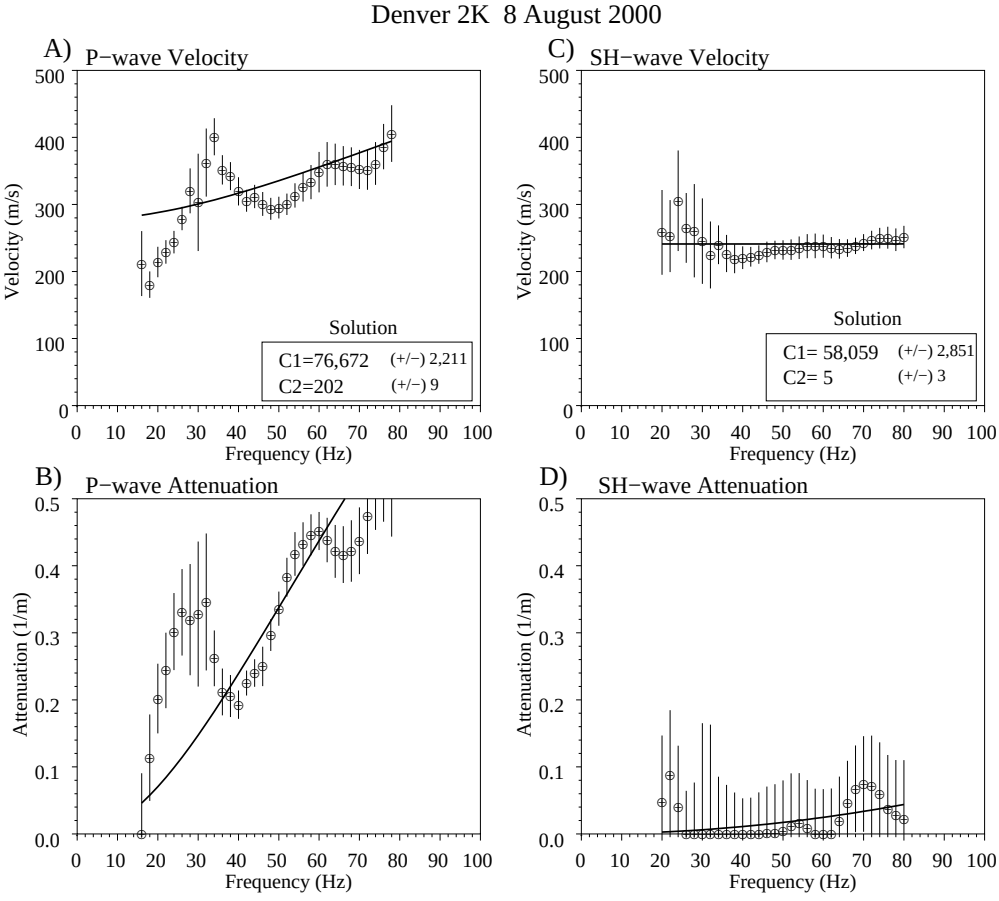

Figure 3. Velocity dispersion and attenuation measurements

doi: 10.1061/40802(189)43

Table 1. Inversion results for P- and SH-waves 1.5< depth <6 meters

Wave Type	C_1 (m^2/s^2)	C_2 (m^2/s)
P-wave	76,672 (+/-) 2,211	202 (+/-) 9
S-wave	58,059 (+/-) 2,851	005 (+/-) 3

very modest compared to determinations made at GeoLogan 1997 (saturated sand, C_2=14 m^2/s) and in Idaho (saturated gravel and sands, C_2 as large as 255 m^2/s) Michaels (1998). While no water content measurements were made at the GeoDenver bore hole, the soil was clearly unsaturated, no water table was observed in the bore hole or neighboring quarry pit.

The compressional P-wave velocity solution shown in Figure 3(a) varies significantly over frequency (from a low of about 300 m/s to a high of 400 m/s). Consistent with a viscoelastic model, the attenuation also varies greatly (from 0 to almost 0.5 nepers per meter). The author has no comparable results for saturated soils, since the Biot type 2 wave generally appears to be present and limits the aperture available for this type of analysis. However, it has long been recognized in the exploration seismic industry that the best signal is returned from reflections when the source is located below the water table (Sheriff and Geldart, 1995, p202). This suggests the possibility that P-waves may differ from S-waves significantly in terms of damping at saturated conditions; greater damping for S-waves, less damping for P-waves.

Comparing Oscillations to Waves, Damping Ratio and Loss Tangent

The equation (1) coefficients C_1 and C_2 are ratios of stiffness and viscosity to density. That is,

$$C_1 = \frac{G}{\rho} \quad C_2 = \frac{\eta}{\rho} \quad , \tag{2}$$

where G is the shear modulus, η is the viscosity, and ρ is the density of the soil (combined matrix and pore fluids). All of the above are specific properties of the soil, they are constants, and they are invariant with frequency. They become lumped parameters when a specific volume of soil is considered (ie. density becomes mass).

Some authors, Kramer (1996), Schnabel et al. (1972), and Stoll (1985), to name just a few, have expressed shear modulus as a complex quantity,

$$G^* = G_R + i\, G_I \quad , \tag{3}$$

where i^2=-1 . The real part, G_R , is frequency invariant, but the imaginary part, G_I, depends on frequency. Specifically,

doi: 10.1061/40802(189)43

$$G_R = \rho C_1 \,, \quad G_I = \rho C_2 \omega = \eta \omega \quad . \tag{4}$$

Loss tangent is given by (Stoll, 1985),

$$\tan(\delta_L) = \frac{G_I}{G_R} = \frac{C_2 \omega}{C_1} \quad , \tag{5}$$

and this is frequency dependent as well. Kramer (1996, p.176-177) and others give damping ratio as

$$\xi = \frac{\eta \omega}{2G} = \frac{C_2 \omega}{2C_1} \quad , \tag{6}$$

from which it can be seen that damping ratio is also frequency dependent. Unfortunately, the vast majority of resonant column reports are for dry samples, and results for shear have revealed damping ratios which appeared to be frequency independent. In an attempt to explain that, Hardin (1965) suggested that viscosity varied with frequency in such a way as to remove the frequency dependence in damping ratio. This new viscosity has been termed "equivalent viscosity" by Kramer. Damping ratios computed from "equivalent viscosity" are not consistent with the Kelvin-Voigt representation, and should not be compared with this work. One should only consider frequency variant determinations of loss tangent or damping ratio when working within a true KV representation.

Shear testing by Stoll (1985) reported loss tangents for frequencies from 2 to 1000 Hz in 20-30 Ottawa sand. The loss tangent for dry sand was largely independent of frequency (.006), but rose significantly with frequency for saturated sand (from .006 to .04). If we substitute Table 1 results for shear into equation (5), we obtain loss tangents for GeoDenver soil which vary from .005 to .054 for the frequency range 10 to 100 Hz. These results suggest that some water was present in the GeoDenver soil, but more detailed conclusions are not possible since neither grains size distributions nor water content were determined.

Beyond the Kelvin-Voigt (KV) Representation for Shear Waves

Figure 4 (a) shows the traditional KV constitutive model as lumped elements in an oscillator. Also shown is how an assemblage of single degree of freedom (SDF) oscillators can be used to represent shear-wave propagation. The KV representation has traditionally been used to mathematically describe the dynamics of soils in engineering practice. Examples include consolidation (ASTM-D2435, 1996) and resonant column (ASTM-D4015, 1996) tests, as well as the response of soils under impact (Roesset et al., 1994). A significant limitation is the single mass element in the model. Soils do not consist of a single component, but are in general a medium consisting of 2 to 3 physical components. These include a solid component and 1 or more pore fluids.

Since the solid and pore fluid elements may move independently of each other, a better model would allow for those possibly separate motions. Pioneering

doi: 10.1061/40802(189)43

work on this topic was done by Biot (1956 a, 1956 b). The essential problem with the KV model is in accounting for the dashpot. Stoll (1985) demonstrated that saturating pores with water produced significantly more viscous damping than was the case for pores filled with air. This observation suggests that damping depends on the pore fluid, and may be due to relative motion between fluid and frame. If the dashpot is to be due to the viscous friction between pore fluids and frame, these materials can not be bound together as a single mass element. Further, even small amounts of water can significantly increase damping values, as reported in studies of lunar soils (Tittmann et al., 1974).

Recent theoretical work by the author has posed an alternative model for saturated media (Michaels, in press). This representation has been named the Kelvin-Voigt-Maxwell-Biot (KVMB) representation, being inspired by those existing models. The lumped element KVMB oscillator is shown in Figure 4 (b). Also shown is how an assemblage of these 2DF oscillators can be constructed to represent shear-wave propagation. In that work, a mathematical mapping between the traditional KV and the KVMB representations is formulated using the decoupling principal (Sadun, 2001).

Air vs. Water as Pore Fluids (Shear)

As can be seen from Figure 4(b), the production of viscous friction through the action of the dashpot depends on the relative motion between pore fluids and the solid frame. This relative motion depends in large part upon the resistance of the pore fluid to motion by virtue of its inertia and the available permeability. The more massive the fluid component, the greater its ability to resist being dragged along with the moving solid frame for a given permeability. The fluid mass increases with both porosity and the density of the fluid. For a given porosity, we should expect a dense fluid to produce greater damping than a less dense fluid, like air. This is what the KVMB model predicts as can be seen in Figure 5. The small level of shear wave damping in the Denver 2000 data may be explained by the lack of inertia for a pore

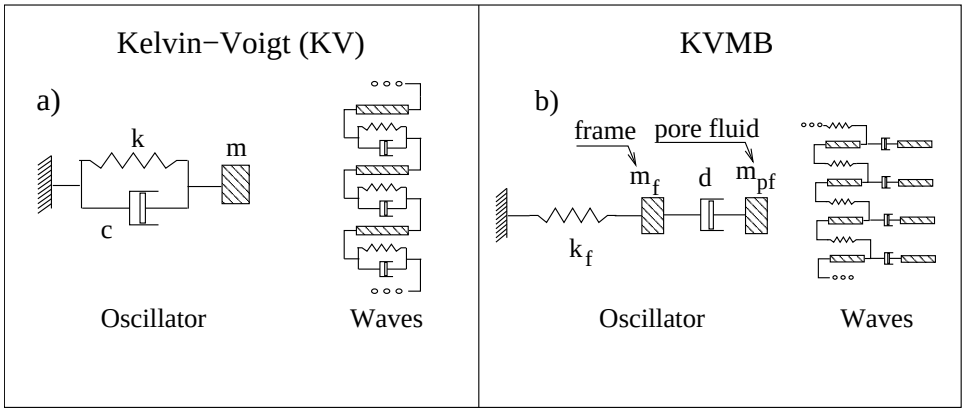

Figure 4. Kelvin-Voigt and KVMB representations of a soil.

doi: 10.1061/40802(189)43

fluid composed largely of air.

The theoretical computation shown in Figure 5 is based on the KVMB representation, and includes an assumption of cylindrical pores, as was the case in Biot (1956a). The vertical axis is an equivalent KV damping ratio mapped from the KVMB representation. The details of this theory for saturated conditions is given in Michaels (in press). The published theory is appropriate for saturated conditions, with either water or air being the fluid completely filling the pore space. The extension to unsaturated conditions is discussed below.

The solid curves in Figure 5 are shown for some selected degree water saturations and the corresponding water contents. The case of completely dry (S=0%) is not shown as it would fall below the chosen axes.

Starting at the left edge of Figure 5 (low frequencies), the pore fluid and frame are largely coupled, moving together. With little relative motion, KV damping is computed to be at a low value. The level of damping increases with frequency as the fluid and frame begin to separate and experience more relative motion due to reduced inertial coupling. The soil is represented by a capillary tube model where all tubes have the same, uniform cylindrical shape and diameter (0.3 mm in this example). This capillary model is the same used by Biot (1956a). Resistance to flow is a result of the fluid viscosity, and this resistance is gradually overcome by inertial forces with increasing oscillation frequency. Maximum KV damping is produced at a peak of the solid curve. Here, the relative motion between frame and fluid is at a maximum, with the frame moving one way and the fluid lagging in phase, moving in an opposite direction producing a large *relative velocity* between the two. As frequency increases, inertial forces dominate. The relative velocity between frame and fluid actually decreases with decreasing absolute velocity of the fluid. That is, in the very

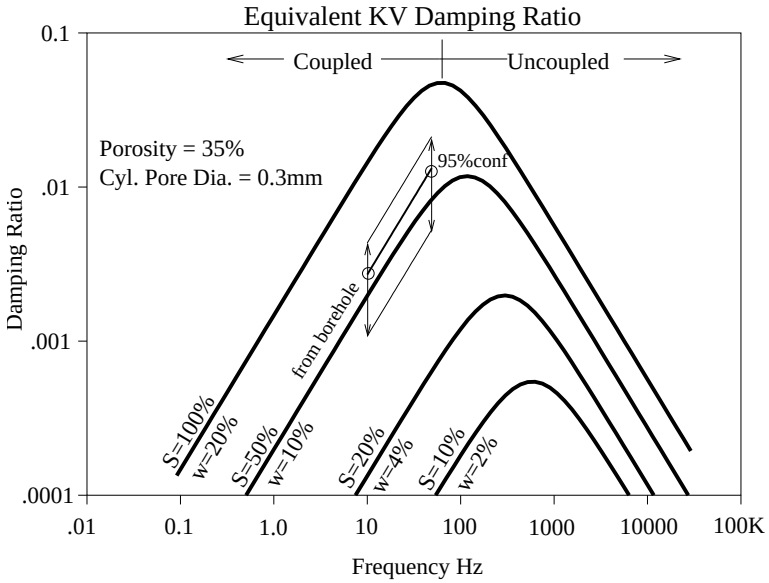

Figure 5. Equivalent KV damping ratio as a function of frequency.

doi: 10.1061/40802(189)43

high frequency limit, the fluid tends to slow down and remain at rest, no longer moving out of phase with the frame. At that point the frame is moving through what is essentially a stationary fluid.

The borehole determined values of C_1 and C_2 (see Table 1) have been converted to damping ratio using equation (6). The borehole computed damping ratios are plotted in Figure 5 between the two circles.

Estimating Damping Ratio for Intermediate Saturations

The computations shown in Figure 5 include estimates of what might be expected at intermediate saturations. The assumptions which lead to the intermediate saturations shown are as follows:

1. Pore fluid mass is a weighted blend of air and water, set by degree saturation.
2. Pore fluid viscosity is a weighted blend of air and water, set by degree saturation.

The equations which implement these assumptions are as follows:

$$m_{fluid} = m_{air} + S m_{water} \quad , \tag{7}$$

$$m_{frame} = m_{solid} + (1 - S) m_{water} \quad , \tag{8}$$

$$\mu_{blend} = (1 - S)\mu_{air} + S\mu_{water} \quad . \tag{9}$$

Here, ***S*** is the degree of water saturation, μ is viscosity, and the masses, ***m***, are computed from porosity and saturations for a relevant volume of interest by the usual method found in any soil mechanics text. In equations (7) and (8), the assumption is that at low water saturations, the moisture clings to the frame and only the air moves relative to the pore throats. At high saturations, the pore fluid flows through the pores by inertia. The extra mass due to water density is essential in creating a significant amount of damping because air, being so light, lacks the needed inertia.

Conclusions

Shear waves appear to have less damping than P-waves in unsaturated soils. This may be due to the relative reduction in pore fluid density that occurs when water is replaced with air, and this results in less inertia to drive fluid flow through pores.

Shear waves are significantly easier to represent than P-waves. The representations shown in Figure 4 are for shear only. The pore fluid (be it air or water) possesses no shear strength, thus requires no spring to represent the fluid component. The situation is quite different in compression, since fluids possess a compressibility (air is highly compressible, water less so).

P-wave damping has been represented by combining volumetric compression of the soil with the diffusion equation (Bardet, 1995). Bardet derives the theoretical

response of a "Biot Column" and predicts the dynamic behavior in terms of several parameters, including soil stiffness, degree of saturation, porosity, specific gravity, and permeability. Since volumetric strain is key to this representation of a soil, Bardet expresses the view that water will not damp a poroelastic shear beam (because no water diffusion is expected in the absence of shear-volume coupling). This view neglects the alternative possibility of inertial coupling in shear.

A summary observation may be this. It appears that, for the case of shear, inertial coupling is the key mechanism by which pore fluids may be driven through the frame. On the other hand, diffusion is the key mechanism by which pore fluids may be driven through the frame in compression. Thus, a low density pore fluid like air can result in high levels of damping for P-waves, but not for SH-waves. A dense pore fluid is required to increase the damping in shear. This is evident when the author compares SH-wave damping in saturated soils with those in unsaturated soils.

Finally, the author's theory predicts that low levels of damping may result even in saturated conditions when the permeability of the soil is either very low or very large. This is because very small pores prevent fluid-frame motion, and very large pores produce less friction when fluid-frame motion occurs. The theory also predicts less damping at very low or very high frequencies as described above. Thus, field observations of shear wave damping may lead to a method for determining permeability of saturated soils, and possibly a method for the estimation of degree water saturation in unsaturated soils.

Acknowledgments

The author would like to express his thanks to Mr. Jeff Farrar for his hard work in organizing the Denver 2000 field day, and to Asphalt Recycling and Stabilization Inc. (ARS) for hosting the field day at their quarry. The author also expresses his thanks to ConeTec and Olson Engineering for the handouts distributed at the field day.

References

American Society of Testing and Materials (SSTM). (1996). “Standard test method for one-dimensional consolidation properties of soils”, D2435, W. Conshohocken, Pa.

American Society of Testing and Materials (SSTM). (1996). “Standard test methods for modulus and damping of soils by the resonant-column method”, D4015, W. Conshohocken, Pa.

Bardet, J.P. (1995). "The damping of saturated poroelastic soils during steady-state vibrations", Applied Mathematics and Comp., 67, Elsevier 3-31.

Biot, M. (1956a). “Theory of propagation of elastic waves in a fluid-saturated porous solid”. I Low-Frequency range”, *J. Acoustical Soc. Am.*, 28(2), 168-178.

Biot, M. (1956b). “Theory of propagation of elastic waves in a fluid-saturated porous solid”. II High-Frequency range”, *J. Acoustical Soc. Am.*, 28(2), 179-191.

doi: 10.1061/40802(189)43

Hardin, B.O. (1965). "The nature of damping in sands." J. Soil Mech. and Found. Div., ASCE, 91(1), 63-97.

Kramer, S.L. (1996). *Geotechnical Earthquake Engineering*, Prentice Hall, New Jersey.

Michaels, P. (1998). "In situ determination of soil stiffness and damping." *Journal of Geotechnical and Geoenvironmental Engineering*, ASCE, 124(8), 709-719.

Michaels, P. (2001). "Use of principal component analysis to determine down-hole tool orientation and enhance SH-waves." *Journal of Environmental and Engineering Geophysics*, EEGS, 6(4), 175-183.

Michaels, P. (in press). "Relating damping to soil permeability", *International Journal of Geomechanics*, ASCE.

Roesset, J., Kausel, E., Cuellar, V., Monte, J., and Valerio, J., (1994). "Impact of weight falling onto the ground", J*ournal of Geotechnical and Geoenvironmental Engineering*, 120(8), 1394-1412.

Sadun, L., (2001). *Applied linear algebra: The decoupling principle*. Prentice Hall, New Jersey.

Sheriff, R.E., and Geldart, L.P. (1995). *Exploration Seismology,* Cambridge University Press, Cambridge England.

Schnabel, B., Lysmer, J. and Seed, H.B. (1972). "Shake, A computer program for earthquake response analysis of horizontally layered sites", *EERC 72-12*, University of California, Berkeley, California.

Stoll, R. (1985). "Computer-aided studies of complex soil moduli", *Proc., Measurement and use of shear wave velocity for evaluating dynamic soil properties,* ASCE, Reston, Va., 18-33.

Tittmann, B.R., Housley, R.M., Alers, G.A., and Cirlin, E.H. (1974). "Internal friction in rocks and its relationship to volatiles on the moon", in *Proc. of the Fifth Lunar Conference,* Supplement 5, Geochimica et Cosmochimica Acta, Vol. 3, 2913-2918.